Supplementary Information

Green and Sustainable Bifunctional Carbonized Wood Electrodes Decorated with Controlled Nickel/α(β)-Nickel(II) Hydroxide to Boost Overall Water Splitting

Jun Yong Yang,‡[a] Jae Gyu Ahn,‡[a] Boemjin Ko,[a] Taeyoung Park,[a] Soon-Jik Hong,[a] Do Kyoung Han,[b,c] Dong Ju Lee,*[d] Cheng Ai Li,*[a] and Sung Ho Song*[a]

[a]Division of Advanced Materials Engineering and Center for Advanced Powder Materials and Parts, Kongju National University, Cheonan, Chungnam 32588, Republic of Korea

[b]Division of Materials Analysis and Research, Korea Basic Science Institute, 169–148, Gwahak-ro, Yuseong-Gu, Daejeon 34133, Republic of Korea

[c]Department of Chemistry, Chung-Ang University, Seoul 06974, Republic of Korea

[d]Department of Advanced Materials Engineering, Chungbuk National University, Chungdae-ro 1, Seowon-Gu, Cheongju, 28644, Republic of Korea

* Corresponding authors.

E-mail addresses: D. J. Lee (dongjulee@chungbuk.ac.kr), C. A. Li (lca12@kongju.ac.kr), S. H. Song (shsong805@kongju.ac.kr).

Experimental Section

Materials and Chemicals

Basswood was purchased from Midwest Products, USA. Nickel chloride hexahydrate ($NiCl_2 \cdot 6H_2O$) and sodium chloride (NaCl) were procured from Samchun Pure Chemical Co., Ltd., South Korea. Potassium hydroxide (KOH) was purchased from Daejung Reagents Chemical, South Korea. All chemicals were of analytical grade and used without further purification.

Fabrication of the CW Electrode

Basswood was directly cut into thin slices perpendicular to the growth direction with sizes of 5 cm × 2.5 cm × 3 mm. The wood samples were washed several times with deionized (DI) water followed by drying at 80 °C. Then, the wood slices were transferred to an Ar-filled quartz tube furnace, carbonized at 1000 °C for 1 h at a heating rate of 15 °C min^{-1}, naturally cooled to room temperature, and removed. After carbonization, the samples were carefully polished with 2000 grit sandpaper to obtain a thickness of 1 mm and repeatedly cleaned with DI water and ethanol by ultrasonic treatment until they were washed out. Finally, the resulting samples were cut into fixed sizes of 2 cm × 1 cm and used as substrates for the electrodeposition of $Ni/Ni(OH)_2$.

Electrodeposition of $Ni/Ni(OH)_2$ on CW

For electrodeposition, cleaned CW, graphite rod, and Ag/AgCl (3 M NaCl) were used as the working, counter, and reference electrodes, respectively, controlled by an electrochemical workstation (BioLogic SP-150 Potentiostat). An electrochemically insulating layer was employed to fix the specific area of the working electrode at 1 cm by 1 cm. In typical synthesis, the CW sheets were immersed in a mixture of $NiCl_2$ (0.1 M) and NaCl (0.1 M) for 1 h by sonication to completely impregnate the pore walls of CW with Ni ions. Electrodeposition was performed via a potentiostatic method at −1.1 V vs. Ag/AgCl at room temperature. After electrodeposition, the as-prepared samples were washed with DI water and dried at room temperature. The obtained electrodes were denoted as $Ni/Ni(OH)_2$/CW-*x* min, where *x* is the deposition time of $Ni/Ni(OH)_2$ in min.

Material Characterization

XRD (MiniFlex 600, Rigaku) was conducted using a Cu radiation source at a scan rate of 5° min^{-1}. Raman spectra were measured using a Raman spectrometer (FEX, NOST, Korea) with 532 nm laser excitation. XPS was performed using an X-ray photoelectron spectrometer (K-

Alpha, Thermo Scientific) to analyze the chemical compositions of the samples. Morphologies and structures of the CW-based electrode samples were examined by SEM (MiRA3-LMH, Tescan) coupled with EDS. TEM was conducted by JEOL JEM-F200 and FEI Tecnai G2 F30 electron microscopes operating at accelerating voltages of 200 and 100 kV, respectively. The TEM samples were prepared by scraping the catalysts from CW followed by sonication in ethanol solution and then dropwise placement on C-coated Cu grids.

Electrochemical Measurements

Electrochemical performances of the electrodes were evaluated by the electrochemical workstation (BioLogic SP-150 Potentiostat) using a three-electrode system with a graphite rod as the counter electrode, Ag/AgCl as the reference electrode, and as-prepared Ni/$Ni(OH)_2$/CW as the working electrode in KOH electrolyte (1.0 M). Before the electrochemical tests, high-purity N_2 was introduced into the electrolyte for 30 min. Polarization curves for HER and OER were obtained via LSV at a scan rate of 5 mV s^{-1} with iR compensation. All reported potentials were calibrated to the reversible H_2 electrode (RHE) according to the equation $E_{RHE} = E_{Ag/AgCl} + 0.209\ V + 0.0591\ pH$. Tafel slopes were calculated from the corresponding LSV curves via linear fitting based on the Tafel equation $\eta = b \log(j) + a$, where j is the gained current density and b is the Tafel slope. Long-term durability tests were performed by chronoamperometric measurements. To estimate the effective ECSAs of the as-prepared electrodes, C_{dl} values were determined by CV of the samples in a narrow potential window from 0.05 to 0.15 V vs. Ag/AgCl at different scan rates ranging from 5 to 60 mV s^{-1}. EIS was conducted in the frequency range from 100 kHz to 1 Hz at a voltage amplitude of 10 mV at 0.05 V vs. Ag/AgCl. Overall, water splitting tests were performed in a two-electrode system, where Ni/$Ni(OH)_2$/CW-10 min served as the cathode and Ni/$Ni(OH)_2$/CW-1 min acted as the anode. LSV curves were assessed between 0.5 and 2.5 V at a scan rate of 5 mV s^{-1} without iR compensation.

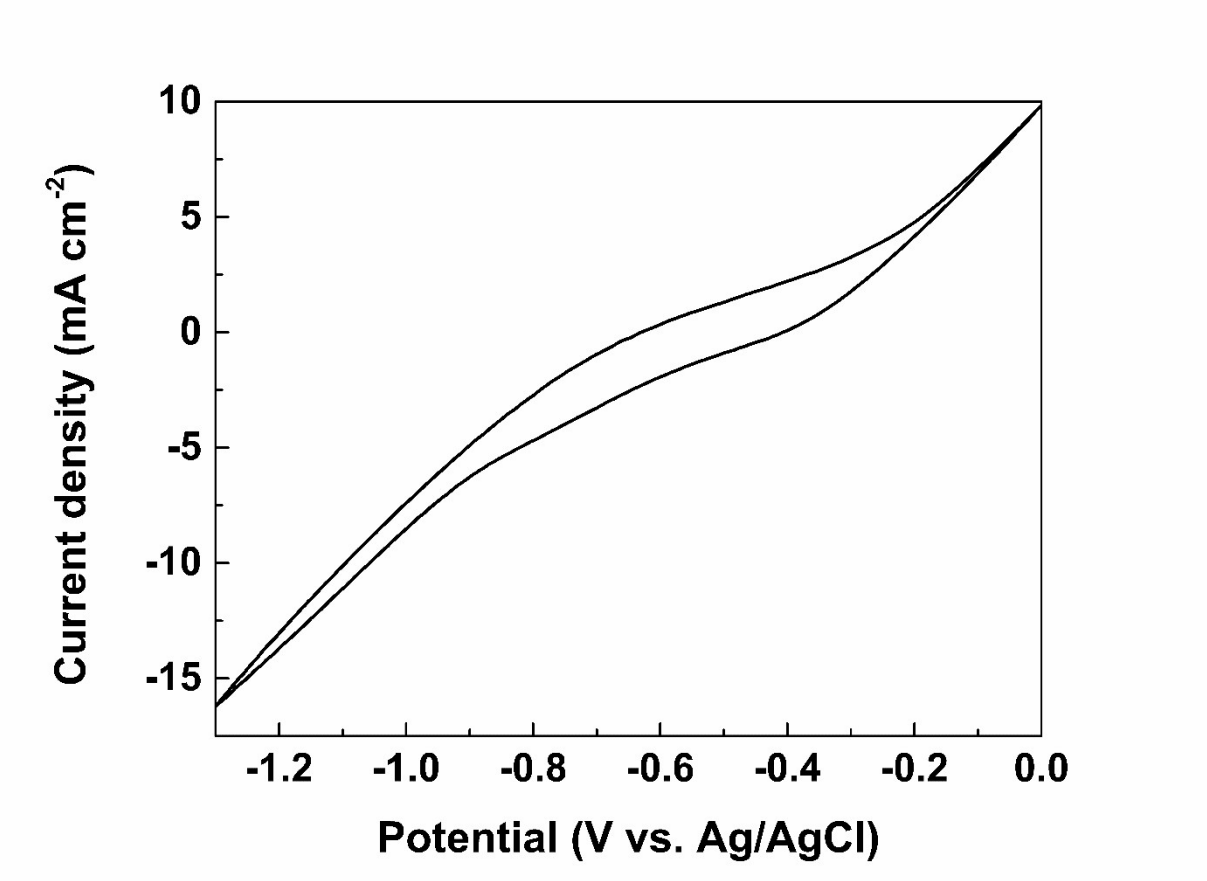

Fig. S1 CV curve of CW electrode in 0.1 M $NiCl_2$ containing 0.1 M NaCl at a scan rate of 10 mV s^{-1}. A broad cathodic peak around the −0.73 V can be assigned to the reduction of nickel.

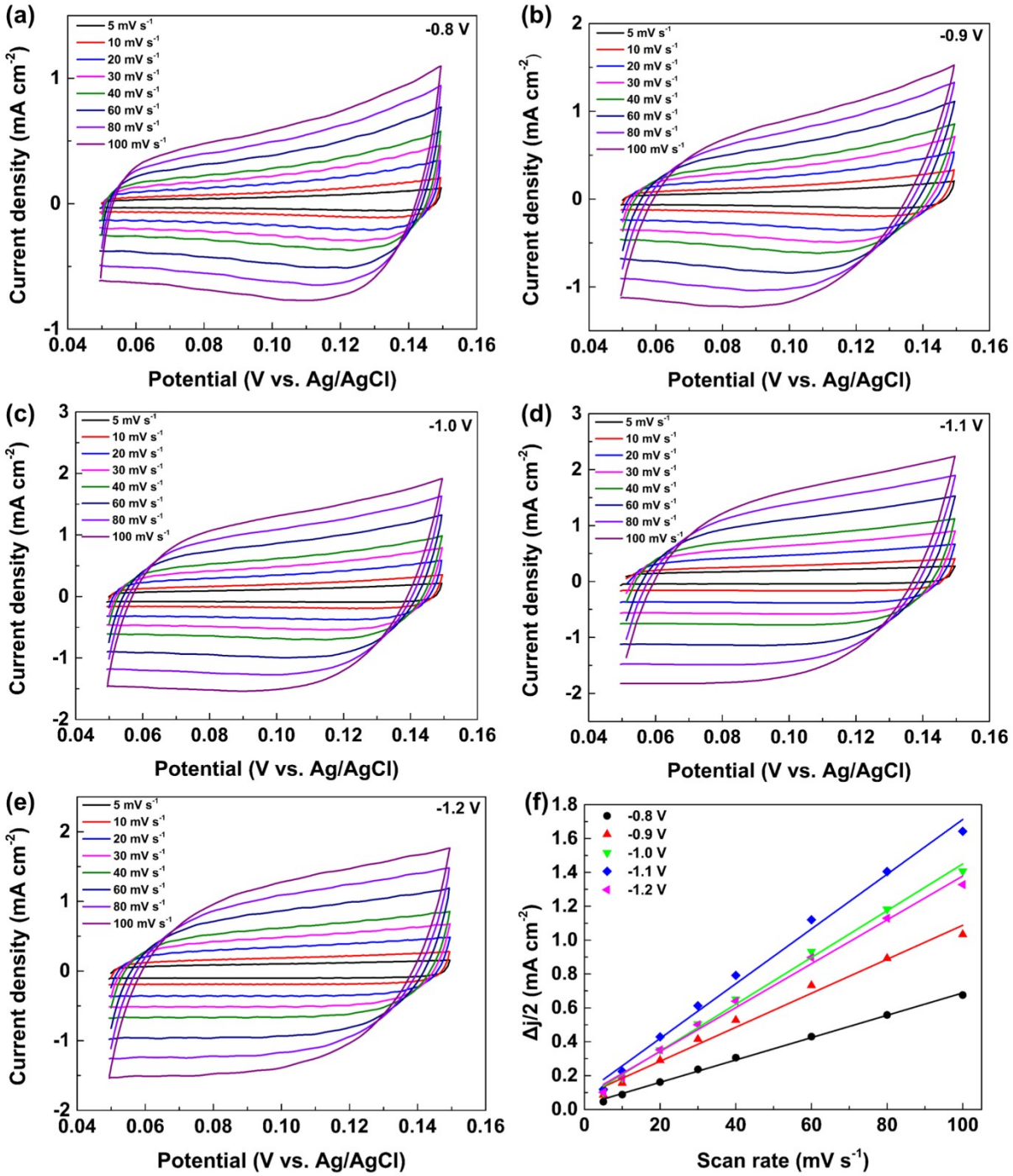

Fig. S2 CV curves in region of 0.05~0.15 V vs. Ag/AgCl for the Ni/Ni(OH)$_2$/CW electrode with deposition potential of (a) −0.8 V, (b) −0.9 V, (c) −1.0 V (d) −1.1 V, and (e) −1.2 V in 1.0 M KOH at various scan rates. (f) Comparison between the C_{dl} values of Ni/Ni(OH)$_2$/CW electrode with different deposition potentials. The linear slope is the C_{dl}, which is used to represent the electrochemically active surface area.

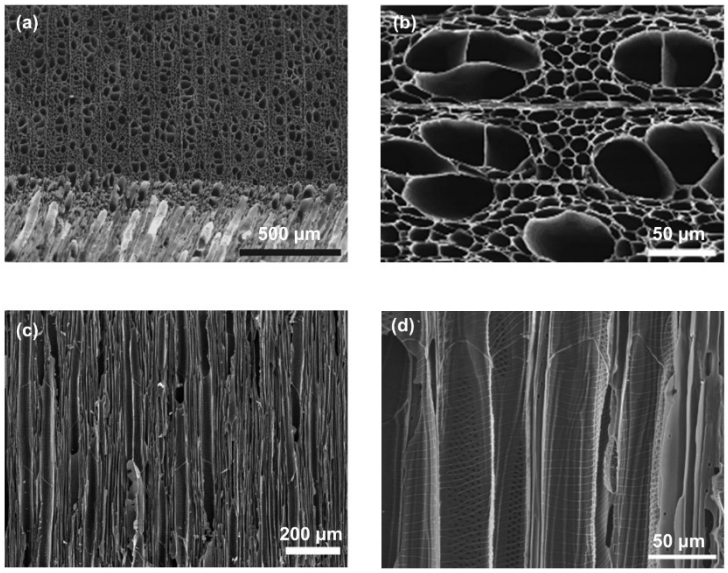

Fig. S3 (a, b)Top-view and (c, d) cross-sectional SEM images of carbonized wood electrode.

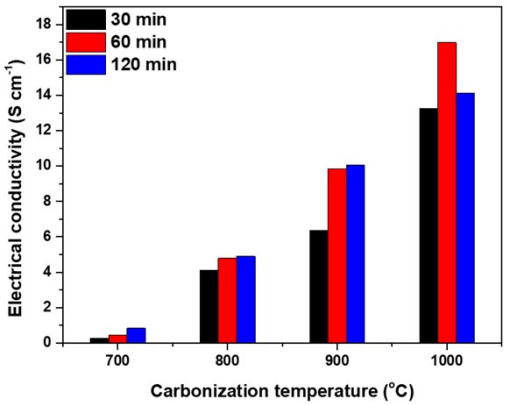

Fig. S4 Electrical conductivities of carbonization woods at different carbonization temperatures and times.

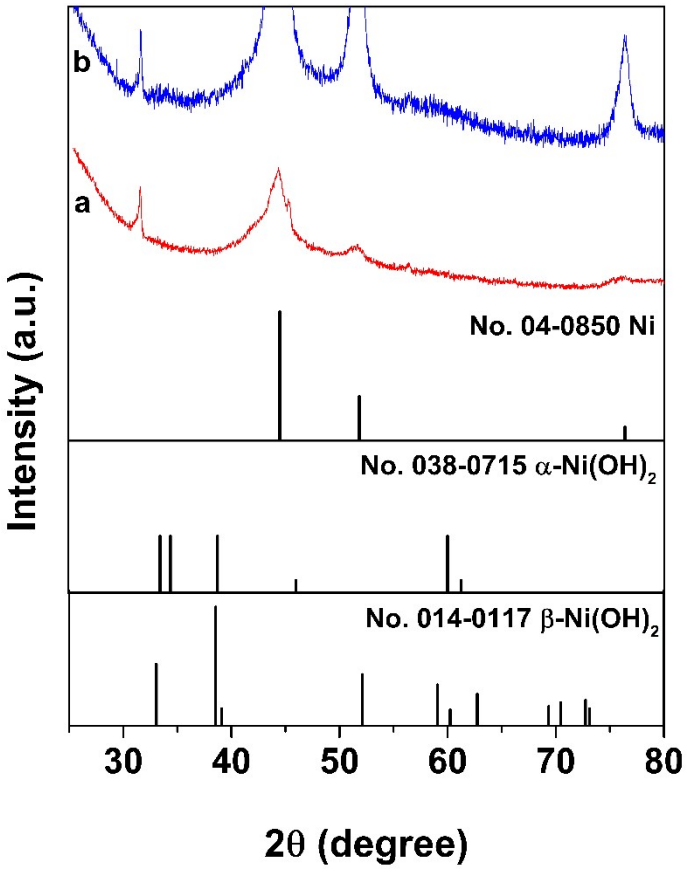

Fig. S5 Magnified XRD patterns of (a) Ni/$Ni(OH)_2$/CW-1 min and (b) Ni/$Ni(OH)_2$/CW-10 min.

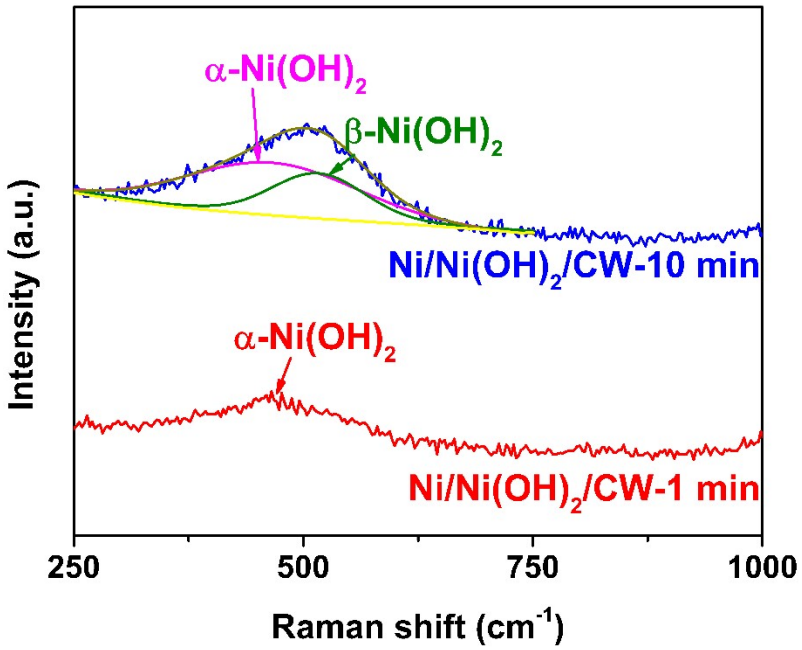

Fig. S6 Magnified Raman spectra of Ni/Ni(OH)$_2$/CW-1 min and Ni/Ni(OH)$_2$/CW-10 min.

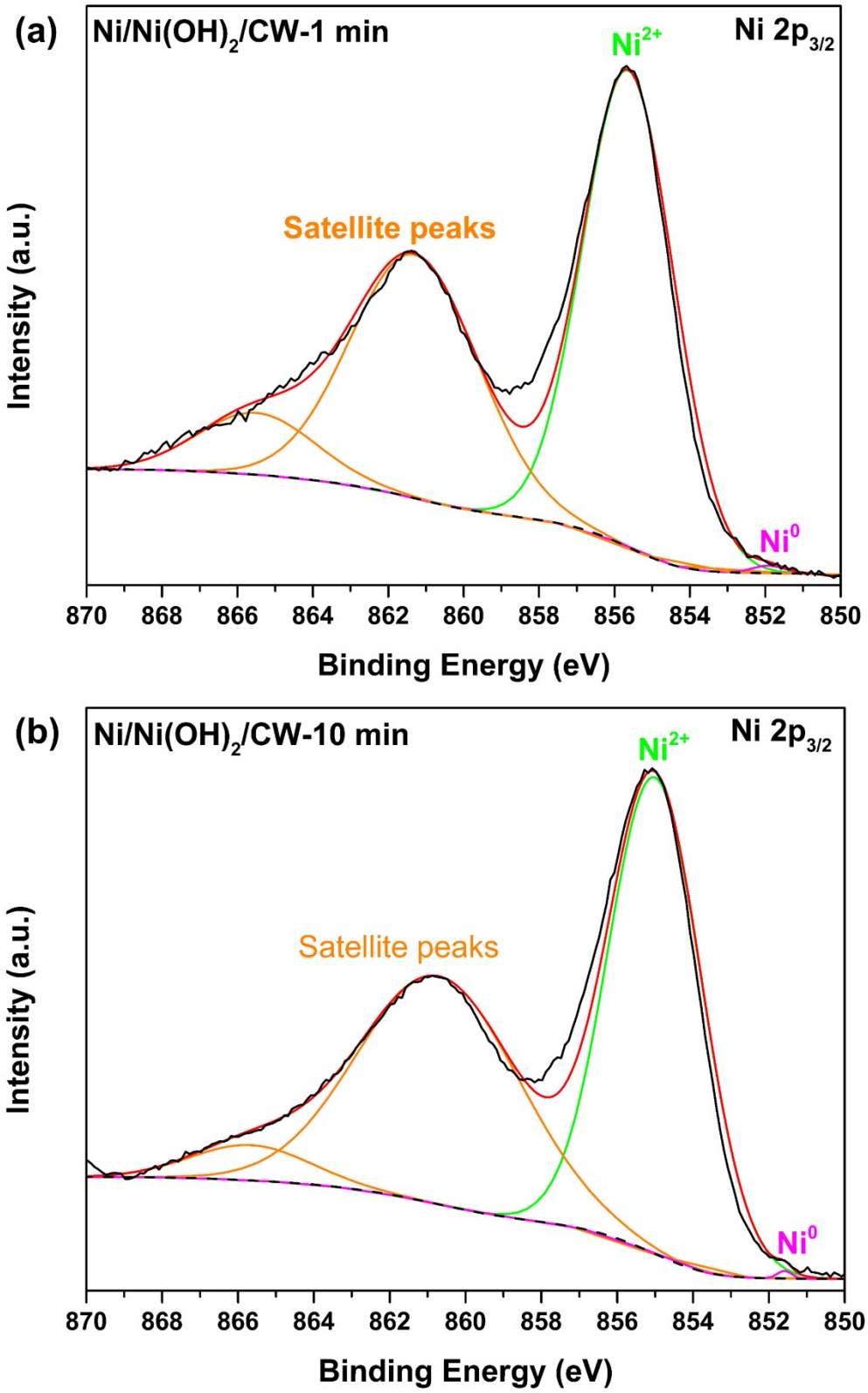

Fig. S7 High-resolution XPS spectra of Ni $2p_{3/2}$ for (a) Ni/Ni(OH)$_2$/CW-1 min and (b) Ni/Ni(OH)$_2$/CW-10 min.

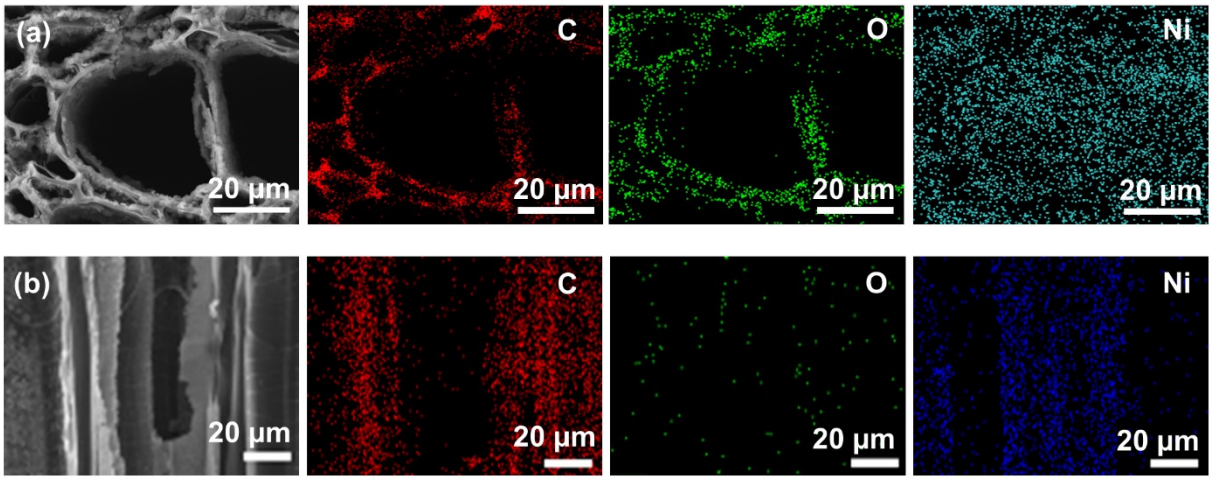

Fig. S8 (a) Top-view and (b) Cross-sectional SEM image of Ni/Ni(OH)$_2$/CW-10 min electrode and the corresponding elemental mapping images.

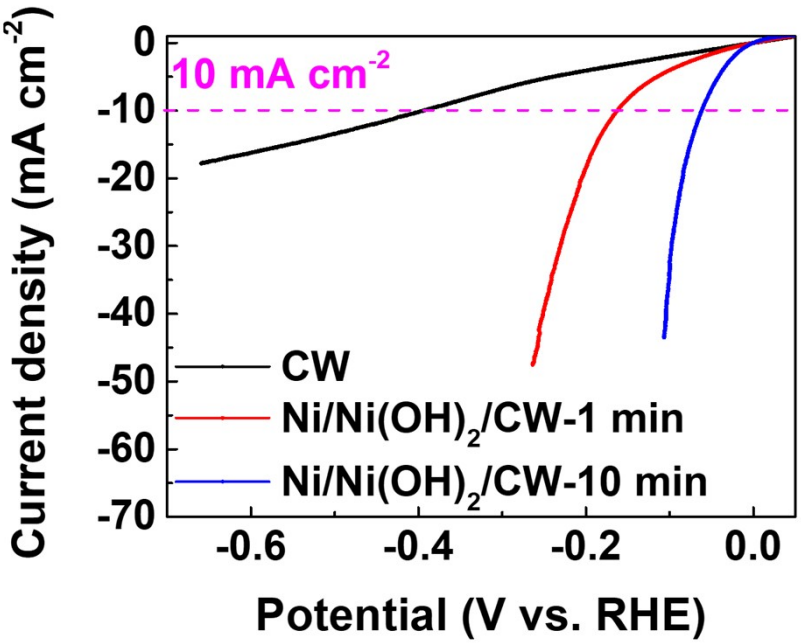

Fig. S9 HER polarization curves of CW, Ni/Ni(OH)$_2$/CW-1 min, and Ni/Ni(OH)$_2$/CW-10 min electrodes with baseline correction.

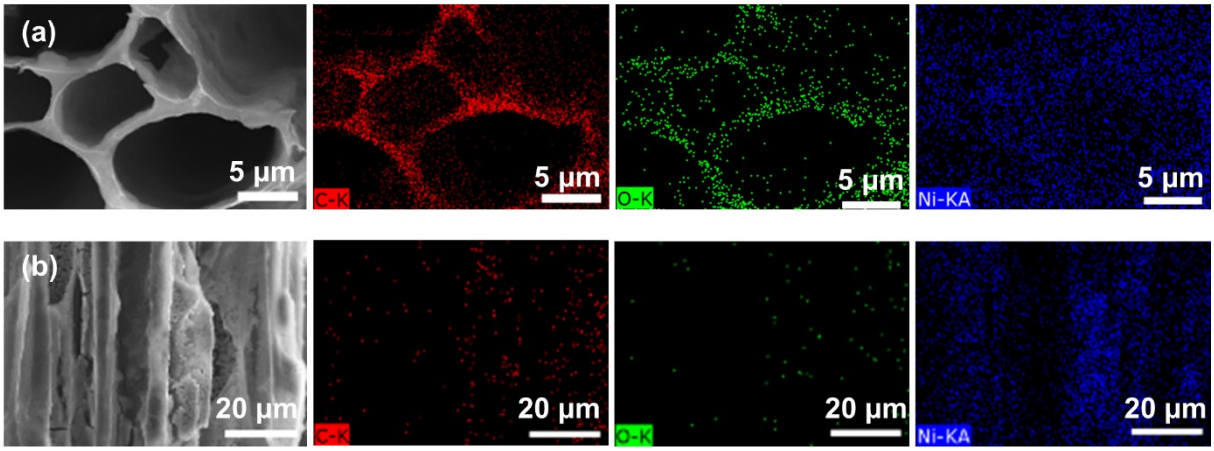

Fig. S10 (a) Top-view and (b) Cross-sectional SEM image of Ni/Ni(OH)$_2$/CW after stability test and the corresponding elemental mapping images of C, O, and Ni distributed on the Ni/Ni(OH)$_2$/CW electrode.

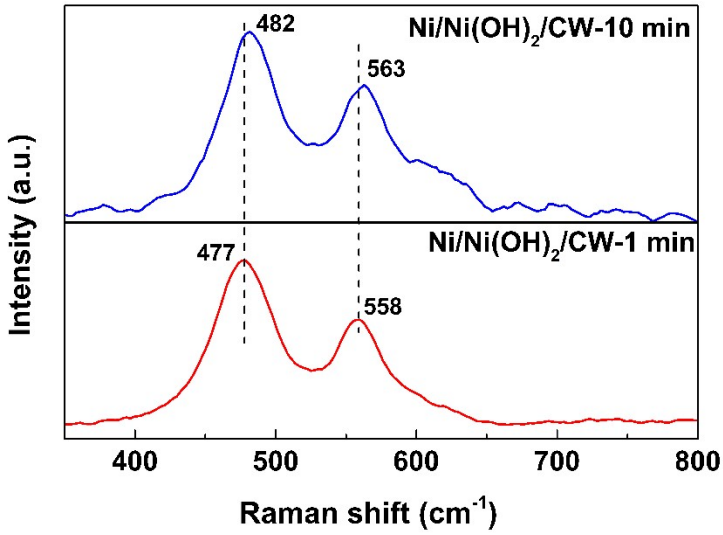

Fig. S11 In situ Raman spectra of Ni/Ni(OH)$_2$/CW-1 min and Ni/Ni(OH)$_2$/CW-10 min electrode at 1.8 V vs. RHE. The measurements were performed in 1.0 M KOH with a Ag/AgCl (3M NaCl) reference electrode, a Pt wire as a counter electrode, and Ni/Ni(OH)$_2$/CW electrode as a working electrode. Chronoamperometry with potential was applied and the acquisition of the Raman measurement followed for 10~30 s.

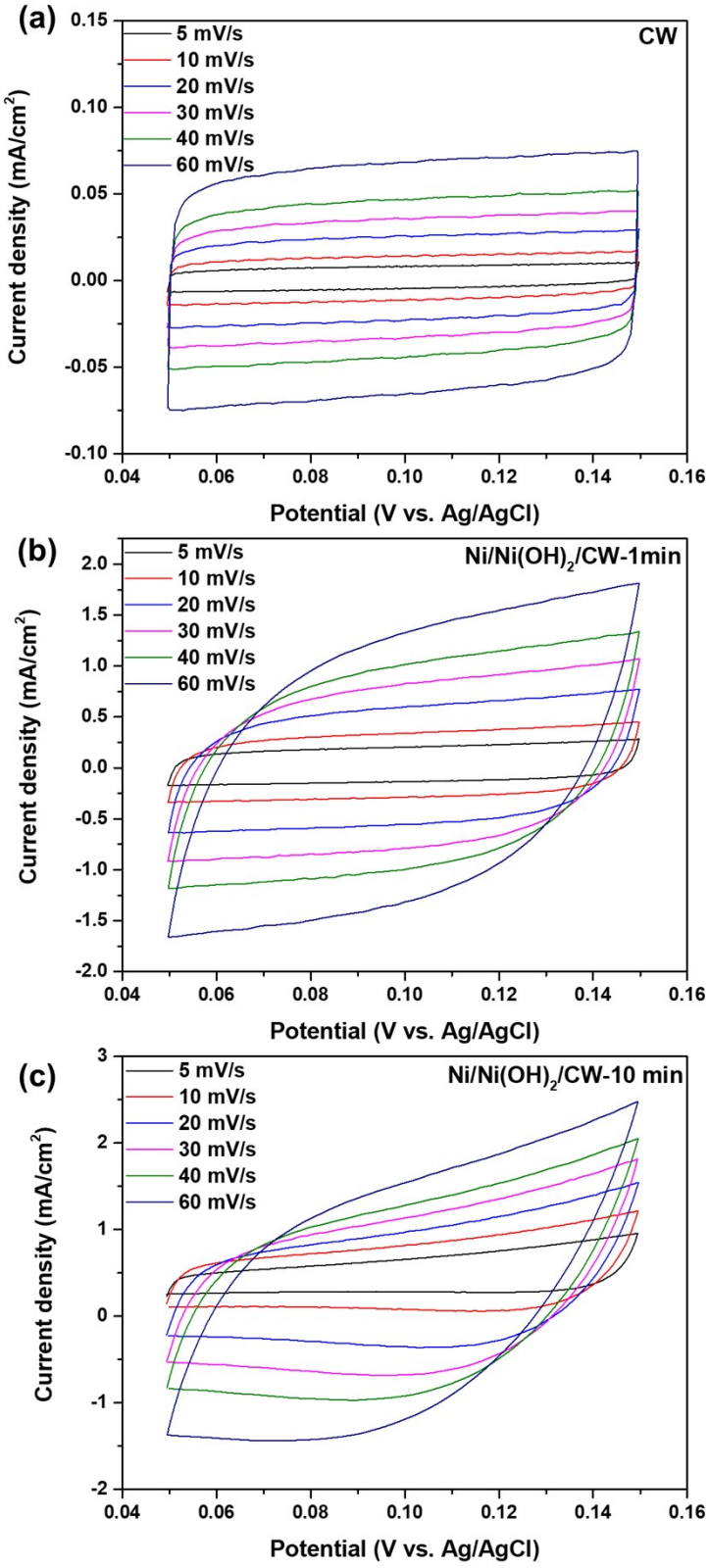

Fig. S12 CV curves of the (a) CW, (b) Ni/Ni(OH)$_2$/CW-1 min and (c) Ni/Ni(OH)$_2$/CW-10 min in the potential region from 0.05 to 0.15 V vs. Ag/AgCl in 1.0 M KOH at various scan rates.

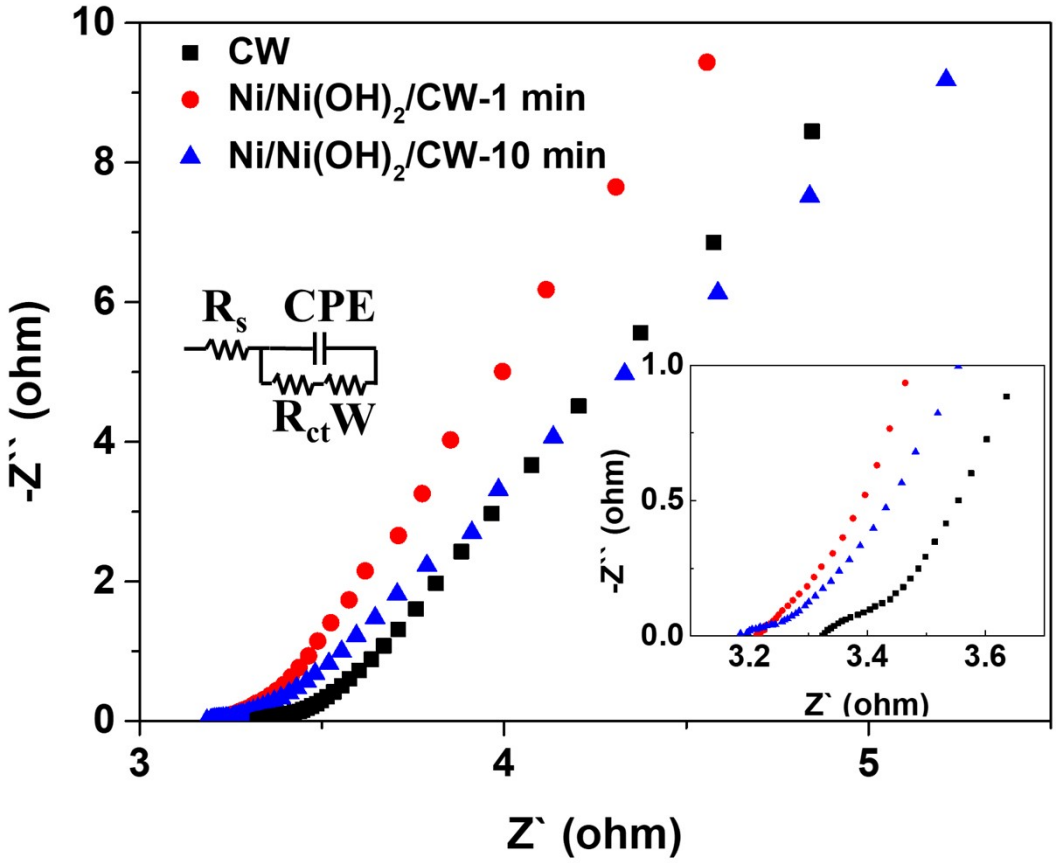

Fig. S13 EIS Nyquist plots of CW, Ni/Ni(OH)$_2$/CW-1 min and Ni/Ni(OH)$_2$/CW-10 min electrodes.

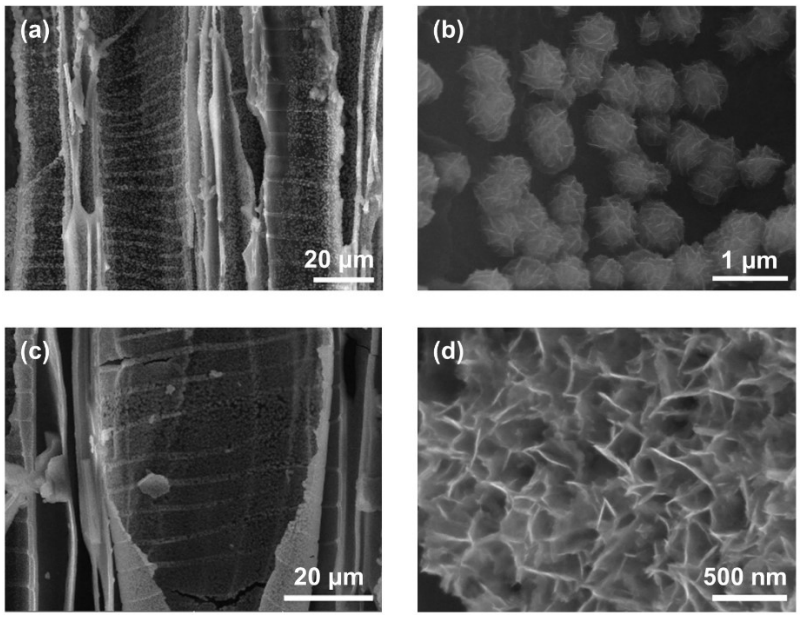

Fig. S14 SEM images of (a, b) Ni/Ni(OH)$_2$/CW-1 min (anode) and (c, d) Ni/Ni(OH)$_2$/CW-10 min (cathode) after stability test.

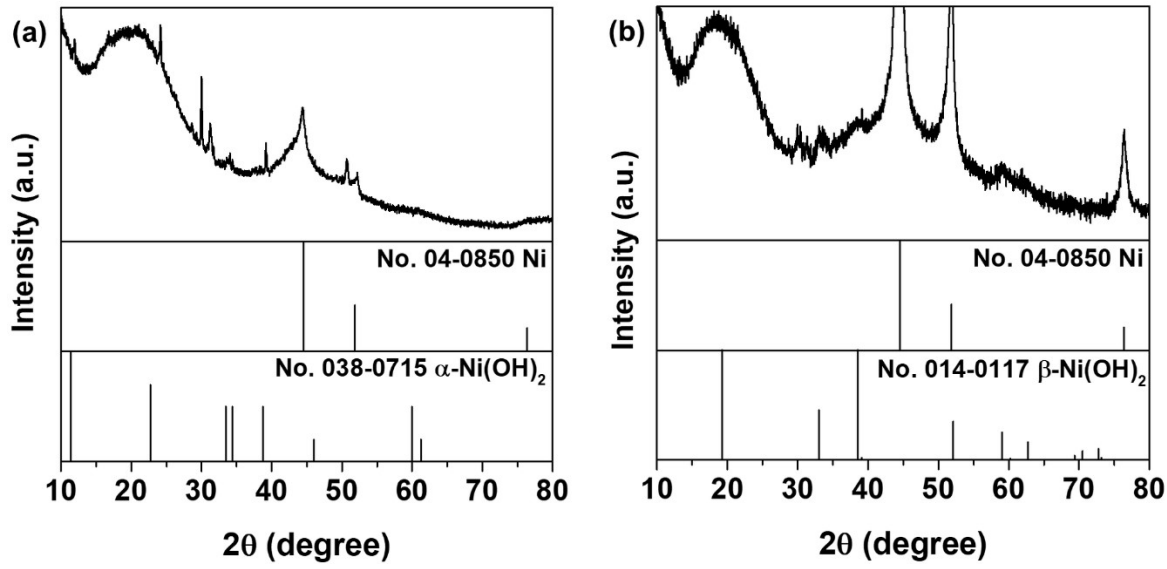

Fig. S15 XRD patterns of (a) Ni/$Ni(OH)_2$/CW-1 min (anode) and (b) Ni/$Ni(OH)_2$/CW-10 min (cathode) after stability test.

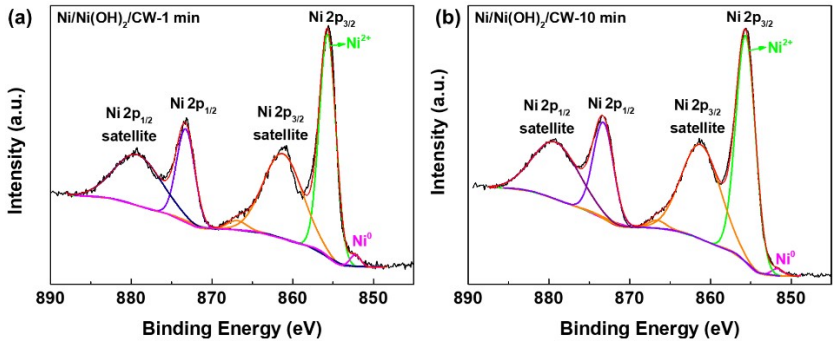

Fig. S16 High-resolution Ni 2p XPS spectra of (a) Ni/Ni(OH)$_2$/CW-1 min (anode) and (b) Ni/Ni(OH)$_2$/CW-10 min (cathode) after stability test.

Table S1 HER activities of various Ni-based electrocatalysts in 1.0 M KOH solution.

Samples	Overpotential (mV) at 10 mA cm^{-2}	Self-supported	Reference
$Ni/Ni(OH)_2$/CW	62	Yes	This work
Co/Ni-CW	157	Yes	Adv. Funct. Mater.,2021,2010951
FeNiP/NWM	108	Yes	J. Energy Chem., 2021, 56, 23
NiP/wood	83	Yes	Electrochim. Acta, 2020, 330, 135274
RuNi-LMH@NCNT/CW	67	Yes	J. Power Sources, 2022, 551, 232219
Pd-NiS/CW	80	Yes	ACS Appl. Mater. Interfaces, 2022, 14, 6818
$Co_{6.25}Fe_{18.75}Ni_{75}O_x$	84	Yes	J. mater. Chem. A, 2018, 6, 167
$NiCo_2N$/NF	180	Yes	ChemSusChem, 2017, 10, 4170
Ni_3Fe-CW	76	Yes	Chem. Eng. J., 2022, 439, 135722
Ni-W-B/wood	46	Yes	Int. J. Hydrogen Energy, 2022, 47, 35571
Co_4Ni_1P NTs	129	No	Adv. Funct. Mater., 2017, 27, 1703455

Table S2 OER activities of various Ni-based electrocatalysts in 1.0 M KOH solution.

Samples	Overpotential (mV) at 10 mA cm^{-2}	Self-supported	Reference
$Ni/Ni(OH)_2$/CW	367	Yes	This work
Co/Ni-CW	330	Yes	Adv. Funct. Mater.,2021,2010951
NiFe-LDHs@Nife/CW	212	Yes	Chem.Eng. J., 2021, 421, 129751
NiFe/CW	259	Yes	Catal. Commun., 2022, 165, 106442
$Co_{6.25}Fe_{18.75}Ni_{75}O_x$	186	Yes	J. mater. Chem. A, 2018, 6, 167
$NiCo_2N$/NF	290	Yes	ChemSusChem, 2017, 10, 4170
NiCo LDH/carbon paper	367	Yes	Nano Lett., 2015, 15, 2, 1421–1427
Ni_3Fe-CW	237	Yes	Chem. Eng. J., 2022, 439, 135722
Ni-W-B/wood	360	Yes	Int. J. Hydrogen Energy, 2022, 47, 35571
α-$Ni(OH)_2$ NP	260	No	ACS Nano, 2018,12, 3875
Co_4Ni_1P NTs	245	No	Adv. Funct. Mater., 2017, 27, 1703455
FeCoNi	288	No	Acs Catal., 2016, 7, 469

Table S3 Comparison of two-electrode water splitting with Ni-based bifunctional electrocatalysts in alkaline media.

Electrode configuration Cathode ‖ Anode	Overpotential (V) at 10 mA cm^{-2}	Self-supported	Substrate	Reference
$Ni/Ni(OH)_2$/CW || $Ni/Ni(OH)_2$/CW	1.74	Yes	Carbonized wood	This work
Co/Ni-CW || Co/Ni-CW	1.64	Yes	Carbonized wood	Adv. Funct. Mater., 2021,2010951
Ni-CW || Ni-CW	1.77	Yes	Carbonized wood	Adv. Funct. Mater., 2021,2010951
$NiCo_2N$/NF || $NiCo_2N$/NF	1.7	Yes	Ni foam	ChemSusChem, 2017, 10, 4170
Ni-W-B/wood || Ni-W-B/wood	1.65	Yes	Carbonized wood	Int. J. Hydrogen Energy, 2022, 47, 35571
Ni_3S_2/NF || Ni_3S_2/NF	1.76	Yes	Ni foam	J. Am. Chem. Soc., 2015, 137, 44, 14023
$NiMoP_2$ || PE-$NiMoP_2$	1.67	Yes	Carbon cloth	J. Mater. Chem. A, 2017, 5, 7191
$NiCo_2O_4$ || $NiCo_2O_4$	1.65	No	Ni foam	Angew. Chem. Int. Ed., 2016, 55, 6290
NiFe-NC || NiFe-NC	1.67	No	Carbon fiber paper	ACS Appl. Mater. Interfaces, 2017, 9, 48, 41906
PO-Ni/Ni-N-CNFs || PO-Ni/Ni-N-CNFs	1.69	No	Ni foam	Nano Energy, 2018, 51, 286.